



## Development of lipid nanoparticle formulations of siRNA for hepatocyte gene silencing following subcutaneous administration



Sam Chen<sup>a</sup>, Yuen Yi C. Tam<sup>a</sup>, Paulo J.C. Lin<sup>a</sup>, Alex K.K. Leung<sup>a</sup>, Ying K. Tam<sup>a,b</sup>, Pieter R. Cullis<sup>a,\*</sup>

<sup>a</sup> Department of Biochemistry and Molecular Biology, University of British Columbia, 2350 Health Sciences Mall, Vancouver, British Columbia, Canada, V6T 1Z3

<sup>b</sup> Acuitas Therapeutics, 2714 West 31st Avenue, Vancouver, British Columbia, Canada, V6L 2A1

### ARTICLE INFO

#### Article history:

Received 7 June 2014

Accepted 25 September 2014

Available online 5 October 2014

#### Keywords:

Lipid nanoparticles

Liposomes

siRNA

Nanomedicine

Subcutaneous administration

Drug delivery

### ABSTRACT

Recently developed lipid nanoparticle (LNP) formulations of siRNA have proven to be effective agents for hepatocyte gene silencing following intravenous administration with at least three LNP–siRNA formulations in clinical trials. The aim of this work was to develop LNP–siRNA systems for hepatocyte gene silencing that can be administered subcutaneously (s.c.). Three parameters were investigated, namely LNP size, residence time of the polyethylene glycol (PEG)–lipid coating and the influence of hepatocyte-specific targeting ligands. LNP sizes were varied over the range of 30 to 115 nm in diameter and PEG–lipid that dissociates rapidly (PEG–DMG) and slowly (PEG–DSG) were employed. In mice, results show that large (~80 nm) LNP exhibited limited accumulation in the liver and poor Factor VII (FVII) gene silencing at 1 mg siRNA/kg body weight. Conversely, small (~30 nm) LNP systems showed maximal liver accumulation yet still had minimal activity. Interestingly, intermediate size (~45 nm) LNP containing PEG–DSG exhibited nearly equivalent liver accumulation as the smaller systems following s.c. administration but reduced FVII levels by 80% at 1 mg siRNA/kg body weight. Smaller systems (~35 nm diameter) containing either PEG–DMG or PEG–DSG were less active; however addition of 0.5 mol.% of a GalNAc–PEG lipid to these smaller systems improved activity to levels similar to that observed for the ~45 nm diameter systems. In summary, this work shows that appropriately designed LNP–siRNA systems can result in effective hepatocyte gene silencing following s.c. administration.

© 2014 Elsevier B.V. All rights reserved.

### 1. Introduction

Recent advances in lipid nanoparticle (LNP) systems for *in vivo* delivery of short-interfering RNA (siRNA) have dramatically improved the potency of siRNA-mediated gene silencing and are undergoing clinical development for the treatment of hypercholesterolemia, transthyretin-mediated amyloidosis and liver cancer [1–3]. Current LNP–siRNA formulations are optimized for activity in the liver after intravenous (i.v.) administration; however there are compelling reasons to develop LNP–siRNA that can be administered subcutaneously (s.c.). These include the potential for self-administration, a prolonged therapeutic window due to a depot effect and access to cell types that are in contact with the lymphatic system, such as immune cells, in addition to tissues available through the circulation. In order to reach distal tissues beyond the local lymph nodes, LNP must drain from the site of injection to the lymphatic system and subsequently enter the arterial circulation [4]. Particle size and polyethylene glycol (PEG) shielding of the LNP influence the drainage and circulation behaviour of s.c. administered liposomes [5–7]. For example, liposomes larger than 120 nm in

diameter were unable to enter the blood compartment whereas those of 40 nm drained almost completely from the injection site and exhibited the lowest regional lymph nodes accumulation [5,6].

Recently, we have developed a microfluidics-based formulation process that permits the straightforward, scalable production of LNP systems over the size range of 20–100 nm in diameter [8–10]. The microfluidic mixing represents a “bottom up” process whereby lipid in ethanol is mixed with aqueous media on a millisecond timescale. The rapid mixing and consequent rapid rise in polarity cause the most hydrophobic components to fall out of solution first, which then act as nucleation sites for subsequent deposition of more polar lipid components [10]. In the case of triolein and 1-palmitoyl-2-oleoyl-sn-glycero-3-phosphocholine (POPC) mixtures, for example, the hydrophobic triolein falls out of solution first to be subsequently coated by the more polar POPC [9]. By changing the ratio of surface lipid (POPC) to core lipid (triolein), LNP with sizes over the range of 20–100 nm can be readily generated. These systems are “limit size” in the sense that they are the smallest possible systems that are compatible with the molecular make-up of the particle.

Similarly, for LNP–siRNA systems, the hydrophobic nucleation site is represented by an inverted micelle formed from association of cationic lipid with the negatively charged siRNA. This is followed by deposition of more polar lipids such as 1,2-distearoyl-sn-glycero-3-phosphocholine

\* Corresponding author at: 2350 Health Sciences Mall, Vancouver, British Columbia, V6T 1Z3, Canada. Tel.: +1 604 822 4144.

E-mail address: [pieterc@mail.ubc.ca](mailto:pieterc@mail.ubc.ca) (P.R. Cullis).

(DSPC) and PEG-conjugated lipid (PEG-lipid) as the polarity of the media is increased further [10].

Because the area per molecule at the lipid–water interface is much larger for a PEG-lipid as compared to DSPC ( $\sim 26 \text{ nm}^2$  vs  $0.6 \text{ nm}^2$ , see [8]) the LNP size is effectively determined by the PEG-lipid to core lipid ratio where the core lipid can be approximated as all the non-PEG lipid in the formulation. Therefore, the proportion of PEG-lipid provides an effective method of regulating LNP–siRNA size, a parameter that may strongly influence gene silencing potency following s.c administration. Here, by varying the PEG-lipid content from 5 mol.% to 0.25 mol.%, we generate LNP–siRNA systems over the size range of 30–115 nm.

Another parameter that may dramatically influence potency is the rate at which the PEG-lipid dissociates from the LNP following *in vivo* administration. As shown previously [11], PEG-lipids with short acyl chain anchors (e.g. 14-carbon ( $C_{14}$ )) dissociate rapidly following injection with a desorption rate of  $\sim 45 \text{ %/h}$ . In contrast, PEG-lipids with 18-carbon ( $C_{18}$ ) acyl chain anchors have a desorption rate of less than 1 %/h. The desorption rate is an important variable in that the PEG-lipid coating determines the circulation lifetime by reducing interactions with and uptake by cells in the body. Thus a PEG- $C_{18}$  (or PEG-DSG) coating gives rise to long circulation lifetimes *in vivo*; however the presence of the PEG-coating prevents uptake by target cells such as hepatocytes and thus compromises gene silencing. Conversely, a PEG- $C_{14}$  (or PEG-DMG) coating that rapidly dissociates promotes LNP association with apolipoproteins such as apolipoprotein E (ApoE) that directly facilitates uptake into hepatocytes via the scavenging and LDL receptor pathway [12–14], resulting in a short lifetime in the circulation. Therefore, the design of LNP–siRNA systems for s.c. administration represents an interesting design problem where a more stable PEG-coating that may be required to allow diffusion from the site of injection could inhibit hepatocyte uptake following arrival in the liver.

As a potential strategy to address this dilemma, a final variable that is considered here involves the use of an N-acetylgalactosamine conjugated PEG-lipid (GalNAc-PEG) as a targeting lipid. GalNAc binds to the asialoglycoprotein receptor found on hepatocytes and induces clathrin-mediated endocytosis [15–18]. For LNP–siRNA systems containing PEG-lipids with long residence times, such a ligand may be expected to assist in hepatocyte-specific LNP uptake. The question then becomes whether such improved uptake results in a material improvement over the uptake and gene silencing resulting from a system with a PEG-lipid shield that dissociates thus allowing the association of serum proteins such as ApoE that promote hepatocyte uptake.

We show in this work that although smaller LNP in the 30 nm size range drain rapidly from the site of s.c injection resulting in relatively high levels in the blood and liver, they exhibit limited gene silencing potency. Conversely, larger systems in the 80 nm size range with rapidly dissociating PEG-DMG do not drain adequately, resulting in limited liver accumulation and gene silencing potency. However, LNP–siRNA systems in the 45 nm size range containing slowly dissociating PEG-lipid represent reasonably potent systems. Interestingly, the potency of the 45 nm systems is not further improved by the addition of GalNAc targeting ligand. However, smaller systems that exhibited enhanced drainage from the injection site and liver accumulation showed improved potency with GalNAc-PEG.

## 2. Methods

### 2.1. Materials

3-(Dimethylamino)propyl(12Z,15Z)-3-[(9Z,12Z)-octadeca-9,12-dien-1-yl]henicosa-12,15-dienoate (DMAP-BLP) [19], (R)-2,3-bis(octadecyloxy)propyl-1-(methoxy poly(ethylene glycol)2000) carbamate (PEG-DMG) [20], (R)-2,3-bis(stearoyloxy)propyl-1-(methoxy poly(ethylene glycol)2000) carbamate (PEG-DSG) and N-acetylgalactosamine cluster conjugated PEG-DSG (GalNAc-PEG)

were provided by Alnylam Pharmaceuticals. 1,2-Distearoyl-sn-glycero-3-phosphocholine (DSPC) was purchased from Avanti Polar Lipids (Alabaster, AL) and cholesterol was purchased from Sigma-Aldrich (St. Louis, MO). The sense and antisense strand sequences of siRNA against Factor VII (siFVII) are 5'-GGAucAucucAAGucuuAct\*<sup>T</sup>-3' and 5'-GuAAGAcuuGAGAuGAucT\*<sup>T</sup>-3, respectively [20–22]. 2'-Fluoro-modified nucleotides are represented in lower case and phosphorothioate linkages are represented by asterisks. siRNAs were provided by Alnylam Pharmaceuticals.

### 2.2. Preparation of lipid nanoparticle-siRNA by microfluidic mixing

DMAP-BLP, DSPC, cholesterol and PEG-DMG were dissolved in ethanol at the mole ratio of 50:10:(39.75 – x):(0.25 + x), respectively where the quantity of cholesterol and PEG-DMG are altered accordingly to  $\pm x$ . siRNA solutions were prepared in 25 mM acetate buffer at pH 4.0. The lipid concentration in ethanol was maintained at 20 mM while the siRNA was at a concentration of 0.37 mg/mL. Lipids and siRNA solutions were then injected into the microfluidic mixer provided by Precision Nanosystems (Vancouver, BC) at a 1:3 volume respectively with a combined final flow rate of 4 mL/min (1 mL/min ethanol, 3 mL/min aqueous). The LNP–siRNA mixtures were immediately dialyzed against a pH 6.7 buffer containing 50 mM MES and 50 mM citrate followed by phosphate buffered saline overnight (12–14 kD MWCO dialysis tubing, Spectrum Labs, Rancho Dominguez, CA). LNP–siRNA were then filtered through a 0.2  $\mu\text{m}$  filter (Pall, Ville St. Laurent, Quebec) and concentrated to approximately 1 mg/mL siRNA using Amicon Ultra centrifugal filters (Millipore, Billerica, MA). The theoretical siRNA-to-lipid ratios for all formulations were maintained at 0.056 mg siRNA per  $\mu\text{mole}$  lipid which results in N/P charge ratios (ratios of the charge on the cationic lipid, assuming that it is in the positively charged protonated form, to the negative charge on the siRNA oligonucleotide) of 3. Formulations that deviated more than 10% from the theoretical target were not used. In experiments requiring radiolabelled LNP,  $^3\text{H}$ -cholesteryl hexadecylether ( $^3\text{H}$ -CHE, Perkin Elmer; Boston, Massachusetts) was incorporated at the ratio of 3.9  $\mu\text{Ci}/\mu\text{mol}$  total lipid. All LNP preparation work was carried out at room temperature.

### 2.3. Analysis of lipid nanoparticles

LNP size and morphology were determined using cryogenic-transmission electron microscopy (cryoTEM) as described previously [8]. LNP size (number weighting) was further confirmed by dynamic light scattering (DLS) using the Malvern Zetasizer NanoZS (Worcestershire, UK). On average, LNP formulations had polydispersity indexes (PDI) below 0.05. Formulations with PDI > 0.1 were not used for further studies. siRNA encapsulation efficiency was determined using the Quant-iT Ribogreen RNA assay (Life Technologies, Burlington, ON). Briefly, LNP–siRNA was incubated at 37 °C for 10 min in the presence or absence of 1% Triton X-100 (Sigma-Aldrich, St. Louis, MO) followed by the addition of the ribogreen reagent. The fluorescence intensity (Ex/Em: 480/520 nm) was determined and samples treated with Triton X-100 represent total siRNA while untreated samples represent unencapsulated siRNA. Total lipid was determined by measuring the cholesterol content using the Cholesterol E assay (Wako Chemicals, Richmond, VA) and the siRNA concentration was determined by measuring the absorbance at 260 nm.

### 2.4. Pharmacokinetics and biodistribution

$^3\text{H}$ -CHE-labelled LNP (based on siRNA concentration) were injected into the s.c. space under the loose interscapular skin at the back of the neck of female CD1 mice (Charles River Laboratories, Wilmington, MA). Mice were euthanized 30 min to 48 h post-injection and tissues were harvested. To determine LNP concentration, approximately 600 mg of tissue or 100  $\mu\text{L}$  of blood was homogenized using the FastPrep

homogenizer from MP Biomedicals (Santa Ana, CA) and incubated with 0.5 mL of Solvable (Perkin Elmer) at 50 °C overnight. Samples were cooled then decolorized with the addition of 200  $\mu$ L of 30% (v/v) hydrogen peroxide followed by the addition of 5 mL of Pico-Fluor Plus scintillation fluid (Perkin Elmer). Samples were read on a Beckman LS 6500 liquid scintillation counter. All procedures were approved by the Animal Care Committee at the University of British Columbia and were performed in accordance with guidelines established by the Canadian Council on Animal Care.

### 2.5. *In vivo* LNP-siRNA activity in the mouse factor VII model

LNP-siRNA were diluted with PBS such that injection volumes were maintained at 10 mL/kg body weight and administered (based on siRNA concentration) s.c. under the loose interscapular skin in 6–8 weeks old female C57Bl/6 mice (Charles River Laboratories, Wilmington, MA). At 1, 2, 4, 7, 11, 15 and 21 days post-injection, 20–30  $\mu$ L of blood was collected from the lateral saphenous vein. On day 28, animals were euthanized and blood was collected via intracardiac sampling. Blood samples were allowed to coagulate at 4 °C overnight and the serum was separated followed by centrifugation for 15 min at 12,000 rpm. The serum FVII levels were determined using the Biophen VII chromogenic assay (Aniara, Mason, OH) according to the manufacturer's protocol.

## 3. Results

### 3.1. LNP-siRNA systems containing PEG-DSG exhibit maximum delivery to liver following s.c. administration

Previous investigations have shown that the diameter of LNP-siRNA systems can be modulated over the range of 25–100 nm by varying the proportion of PEG-lipid in the formulation using a microfluidic mixing process [8]. As the lipid composition employed here is different than used previously, we examined the size distribution achieved for LNP-siRNA systems composed of DMAP-BLP, DSPC, cholesterol and PEG-DMG in the molar ratios 50:10:(39.75 - x):(0.25 + x), where x was varied from 0 to 4.75, encapsulating siRNA at a N/P (+/-) charge ratio of 3. The total amount of PEG-lipid was therefore varied from 0.25 to 5.0 mol.%. The size and structure of these LNP-siRNA systems were determined by cryoTEM and DLS (Fig. 1). LNP-siRNA systems of sizes ranging from 30 nm to 115 nm in diameter were generated that exhibited electron dense cores as previously described [8,10] (Fig. 1 A–D). Particle sizes determined using DLS were consistent to those determined using cryoTEM (Fig. 1E). Size differences compared to previous reports [8] can be attributed to the different lipid compositions employed. Hereafter for simplicity, reported particle sizes are rounded to the nearest multiple of five and based on DLS measurements.

Previous studies have shown that particle size can affect liposome drainage and biodistribution following s.c. administration [4,5]. In order to investigate the impact of LNP-siRNA size on the accumulation at the local draining lymph nodes, LNP-siRNA of either ~30 nm or ~80 nm in diameter were radiolabelled with trace amounts of the non-exchangeable <sup>3</sup>H-CHE [23] and administered s.c. at 1 mg/kg in the inter-scapular region of mice. The axial and brachial lymph nodes were collected and analyzed for residual LNP (Fig. 2). While no significant difference in brachial lymph node accumulation was observed over 24 h, approximately five times more ~30 nm LNP (~2.5% injected dose) was detected in the brachial lymph nodes compared to the larger ~80 nm particle (~0.5% injected dose) by 48 h post administration. Not surprisingly, very little (less than 0.1% injected dose) of either formulation was detected in the axial lymph nodes (data not shown) since the inter-scapular site of injection drains almost exclusively to the brachial lymph nodes [24].

In order to investigate the impact of particle size and PEG coating on the distribution of s.c. administered LNP-siRNA to blood and

subsequently to the liver, radiolabelled LNP-siRNA were tracked for 48 h post s.c. injection. PEG-lipids containing either the rapidly dissociating C<sub>14</sub> (PEG-DMG) or the non-dissociating C<sub>18</sub> (PEG-DSG) acyl anchors were tested. As shown in Fig. 3A, the small systems containing 5% PEG-DSG exhibited by far the highest circulating concentration (C<sub>max</sub>) of LNP (17.1% of the injected dose) following s.c. administration (Table 1). However, this did not result in higher levels of accumulation in the liver. Instead, equivalent levels of accumulation corresponding to approximately 15% of the total dose were observed 48 h post injection for small (~30 nm) LNP containing either 5% PEG-DMG or PEG-DSG (Fig. 3B). Furthermore, these levels were equivalent to those observed for large (~80 nm) and intermediately sized (~45 nm) LNP with PEG-DSG. The fact that the small LNP containing 5% of the non-exchangeable PEG-DSG do not exhibit greater liver accumulation despite achieving a higher maximum concentration in the blood can be attributed to their long circulation lifetimes following penetration to the

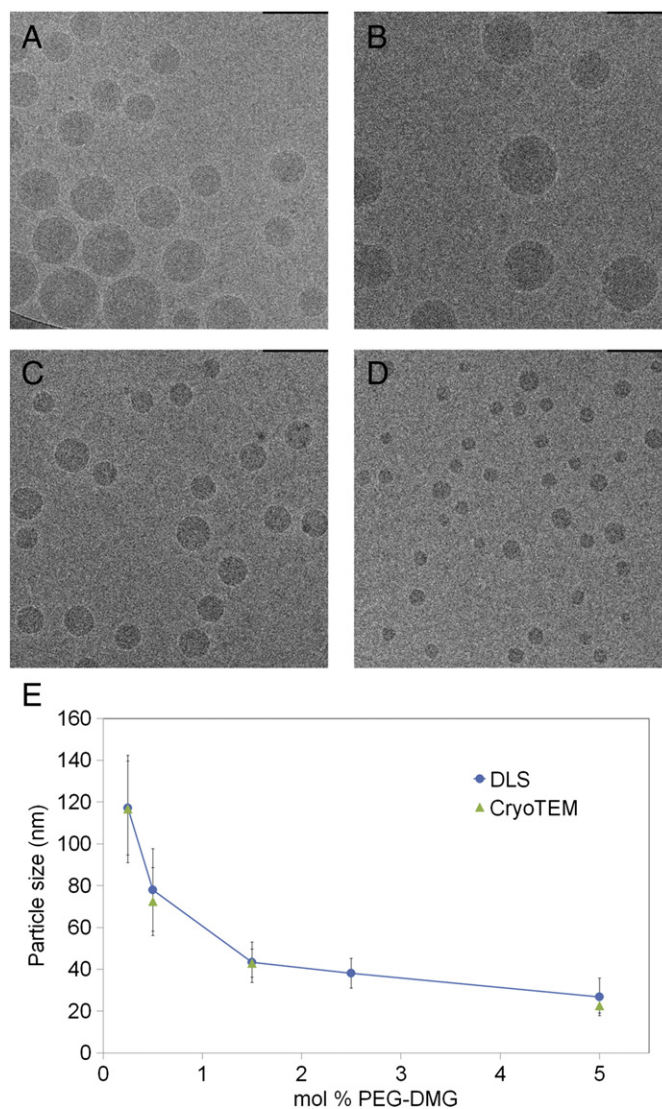


**Fig. 1.** LNP size is correlated with amount of PEG-lipid. LNP of various sizes were made using microfluidics by varying PEG-DMG content. (A–D) Representative cryoTEM micrograph of LNP containing PEG-DMG at 0.25 mol.% (A), 0.5 mol.% (B), 1.5 mol.% (C) and 5 mol.% (D) were shown. (E) Size and polydispersity of LNP formulations in A–D were determined using cryoTEM images and DLS. Sizes determined by cryoTEM for LNP containing 0.25, 0.5, 1.5 or 5 mol.% PEG-DMG were 117, 78, 43 and 23 nm respectively. By DLS, LNP containing 0.25, 0.5, 1.5, 2.5, or 5 mol.% PEG-DMG were 117, 78, 43, 37, and 28 nm respectively. Results shown represent the mean diameter  $\pm$  s.d. of ~200 LNP for cryoTEM and 3 independent formulations for DLS. Scale-bar represents 200 nm in A and 100 nm in B–D.

blood compartment which facilitates distribution to tissues other than the liver [25–27]. At the maximum concentration of LNP appearing in the blood, no hemolysis-induced toxicity is expected since LNP–siRNA showed no hemolytic activity at pH 7.4 (Supplemental Fig. 1). Less than 5% of the ~45 nm and ~80 nm PEG–DMG LNP was found in the liver.

### 3.2. Intermediate sized (45 nm) LNP–siRNA systems exhibit maximal hepatic gene silencing following s.c. administration

We next investigated the effect of LNP size on hepatocyte gene silencing upon s.c. administration. Experiments were performed to compare LNP ranging from ~30 nm to ~100 nm in diameter with either the rapidly dissociable PEG–DMG (Fig. 4A) or the more stable PEG–DSG (Fig. 4B). Animals were injected s.c. with LNP loaded with siRNA against FVII, a protein produced and secreted by hepatocytes, at 1 or 5 mg/kg siRNA. Serum FVII levels were determined 48 h post injection. While the largest LNP tested showed no gene silencing at the 1 mg/kg dose, 5 mg/kg siRNA induced a 40% reduction in protein levels in animals treated with PEG–DSG LNP but not PEG–DMG LNP. Since the PEG–DSG LNP were approximately 15 nm smaller than the PEG–DMG counterpart, it is unclear whether this improvement in gene silencing was a result of size or the PEG–lipid. On the other end of the size spectrum, LNP of diameter ~30 nm composed of 5 mol.% of either PEG–lipid were unable to silence FVII regardless of the injected dose. Interestingly, the most potent LNP for either PEG–lipid were those with intermediate diameters (~45 nm). We observed that FVII levels were reduced by 60% and 80% at 1 mg/kg and 90% and 95% at 5 mg/kg for PEG–DMG LNP and PEG–DSG LNP, respectively. These results suggest that hepatic gene silencing via s.c. administration requires LNP of a specific size which, in the case of these particles, is ~45 nm.

To explore the duration of gene silencing following s.c. administration, blood was collected from animals injected with the most active LNP–siRNA formulation (~45 nm diameter) over 28 days and serum FVII levels were determined (Fig. 5). A single injection of 1 mg/kg led to greater than 50% FVII protein reduction which persisted for at least 4 days for PEG–DMG LNP and 7 days for PEG–DSG LNP (Fig. 5A). This result implicates the importance of a stable PEG coat for gene silencing using LNP administered s.c. The higher hepatic gene silencing ability of PEG–DSG LNP can be attributed, at least in part, to the fact that they accumulated at least 3-fold more in the liver than PEG–DMG LNP of a similar size (Fig. 3B). When the mice were dosed at 5 mg/kg, a reduction in FVII of approximately 90% was observed for a minimum of

4 days and protein levels were reduced below 50% for at least 11 days (Fig. 5B). There was no significant difference in the degree or duration of silencing between LNP containing PEG–DMG or PEG–DSG likely due to fact that the dosage was high enough to mask any potency differences.

It is surprising that small ~30 nm LNP with the stable PEG–DSG coat were less active in gene silencing given that they showed favourable blood exposure and liver accumulation. We speculated that the reduced gene silencing was likely the result of inadequate uptake of LNP into hepatocytes since the stable PEG–DSG coat has been shown to inhibit opsonization in circulation and delay LNP clearance to the liver. In order to explore this possibility, GalNAc conjugated PEG–lipid (GalNAc–PEG) that targets asialoglycoprotein receptor expressed on the surface of hepatocytes was used as a targeting lipid [12]. Two PEG–DSG LNP compositions resulting in approximately 45 nm and 35 nm in diameter were tested with or without GalNAc–PEG lipid. Interestingly, no significant improvement on activity was observed at 48 h post administration when 0.5 mol.% GalNAc–PEG was incorporated into 45 nm LNP (Fig. 6A). This is not surprising since these formulations were the most active as shown in Fig. 4 and were likely able to utilize ApoE-mediated endocytosis. However, when 0.5 mol.% of GalNAc–PEG was incorporated into the smaller ~35 nm PEG–DSG LNP, a dramatic improvement in FVII silencing was observed (Fig. 6B). Targeted LNP (containing GalNAc–PEG) showed almost 90% FVII knockdown for at least 7 days whereas only ~50% protein reduction was observed using non-targeted LNP. Furthermore, the duration and degree of gene silencing of GalNAc–PEG LNP was similar to PEG–DMG LNP.

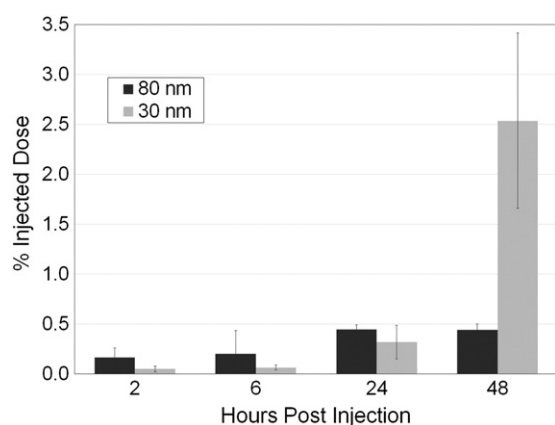


**Fig. 2.** A greater proportion of small LNP accumulate at brachial lymph nodes following s.c. administration. <sup>3</sup>H-labelled LNP containing PEG–DSG that were ~80 nm (black) and ~30 nm (grey) in diameter were administered s.c. at 1 mg/kg body weight. Brachial lymph nodes were harvested at 2, 6, 24 and 48 h post injection. Results shown represent the mean  $\pm$  s.d. of four animals.

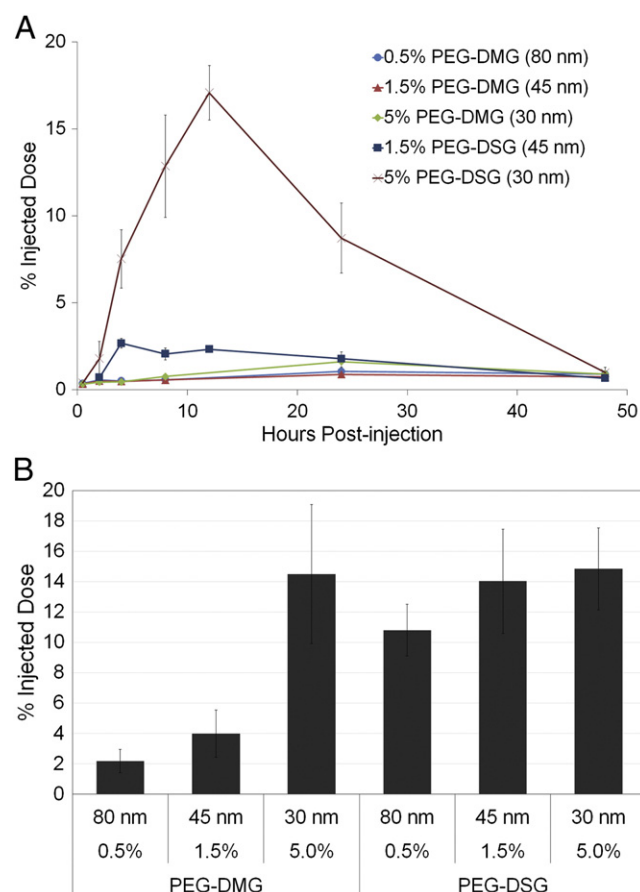


**Fig. 3.** LNP with non-dissociating PEG coating drain more quickly into the blood and exhibit enhanced accumulation in the liver following s.c. administration. <sup>3</sup>H-CHE labelled LNP containing 0.5%, 1.5%, 5% PEG–DMG, 1.5% or 5% PEG–DSG were administered s.c. at 1 mg/kg of body weight. Blood and livers were collected at various time points. (A) Clearance of LNP from blood over a period of 48 h. (B) Amount of LNP found in liver at 48 h. Results shown represent the mean  $\pm$  s.d. of four animals.

**Table 1**

Area-under-curve (AUC) and maximum blood concentration ( $C_{max}$ ) of LNP with varying sizes.

LNP	Size (diameter, nm)	AUC (% inj. dose h)	$C_{max}$ (% injected dose)
0.5% PEG-DMG	80	39.0	1.0 ± 0.2
1.5% PEG-DMG	45	33.6	0.9 ± 0.1
5% PEG-DMG	30	51.6	1.6 ± 0.6
1.5% PEG-DSG	45	75.3	2.7 ± 0.3
5% PEG-DSG	30	376.1	17.1 ± 1.6

#### 4. Discussion

To our knowledge, this is the first report on s.c. administration of LNP–siRNA for *in vivo* gene silencing. It was hypothesized that particle size and PEG steric barrier are crucial factors in determining the potency of s.c. administered LNP–siRNA since the particles must traverse through the meshwork of loose connective tissue to reach the local lymph nodes and drain into the lymphatic system and subsequently into the peripheral circulation. Consistent with this hypothesis, it was found that small LNP–siRNA with a stable PEG coat had a much greater AUC in blood (Table 1) than other formulations tested indicating that they were made available to access tissues such as the liver. We also demonstrated the importance of the stability of the PEG coat and particle size on the potency of s.c. administered LNP–siRNA. We discuss the implications of this study for the development of next generation LNP–siRNA systems with improved potency following s.c. administration.

The utility of liposomes as small as 40 nm in diameter for s.c. administration has been previously explored; however, these were bilayer

systems manufactured by sonication and are poorly suited for carrying a therapeutic payload such as siRNA [6,28]. For the non-bilayer “solid core” LNP–siRNA systems described here [8,10], an inverse relationship between LNP size and the ability to drain from the site of injection and enter the blood following s.c. administration was observed. This is consistent with previous literature indicating that smaller LNP are able to drain faster into the circulation than their larger counterparts [4,6]. At the brachial lymph nodes where the s.c. injected LNP are expected to drain to, ~2.5% of the small (~30 nm) PEG-DSG LNP was detected 48 h following s.c. administration, compared to only <0.5% of the larger (~80 nm) LNP (Fig. 2). This suggests that the larger PEG-DSG LNP remain at the site of injection and slowly permeate into the circulation, whereas the small PEG-DSG LNP reach the lymph node at a faster rate resulting in a greater accumulation at the lymph node and subsequent release into the circulation. This is also supported by our observation that large and small LNP exhibit low and high  $C_{max}$  in blood, respectively (Fig. 3A and Table 1).

For all LNP containing the rapidly dissociable PEG-DMG, the maximum dose appearing in the blood was less than 2% of the total injected dose (Fig. 3A and Table 1). This low  $C_{max}$  may be the result of the PEG-DMG lipid being rapidly dissociated from the LNP leading to insufficient steric barrier necessary for the LNP to avoid immune clearance or particle aggregation, both of which could result in a build-up of LNP at the injection site and cause local toxicities. Any quantity that reaches the peripheral circulation will be rapidly cleared by the liver because PEG-DMG LNP administered i.v. have a circulation lifetime of less than 1 h [11]. It is estimated that less than 5% of the ~45 and ~80 nm

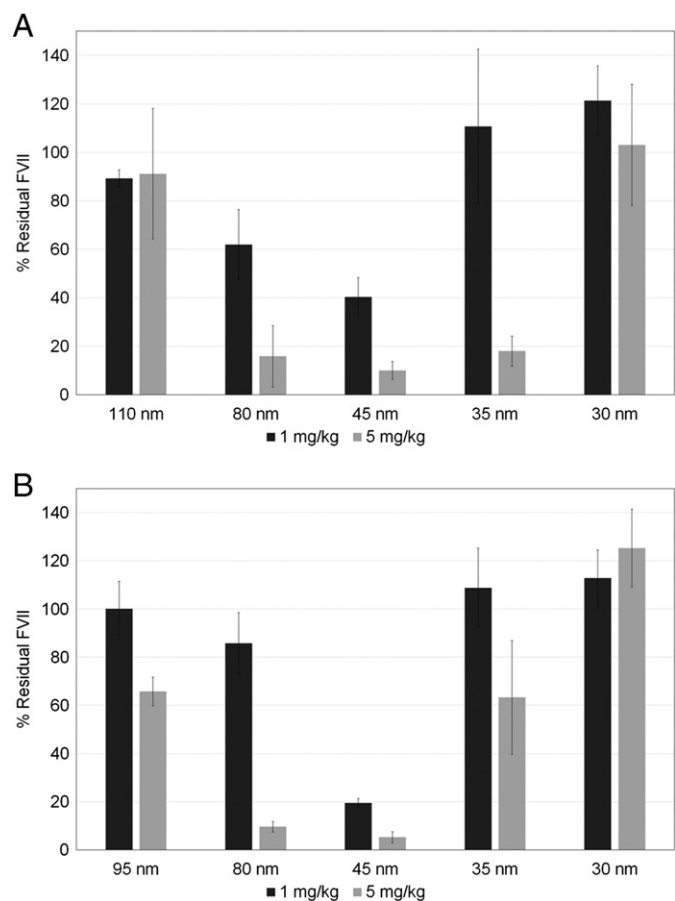


**Fig. 4.** ~45 nm LNP exhibit maximum gene silencing post s.c. injection. (A) PEG-DMG or (B) PEG-DSG LNP were s.c. administered at 1.0 (black) or 5.0 mg/kg (grey) of body weight and the serum FVII was determined 48 h post-injection. Results shown represent the mean ± s.d. of four animals.

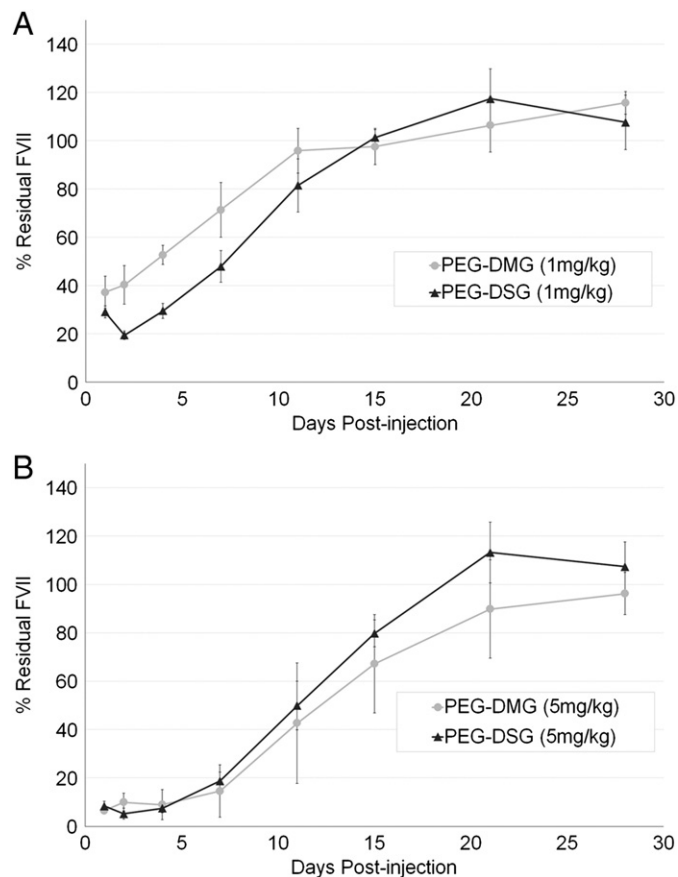


**Fig. 5.** Persistent gene silencing (<50% protein) is observed over 11 days following s.c. administration of ~45 nm diameter LNP. LNP of similar sizes (~45 nm) but different PEG-lipids were administered s.c. in C57Bl/6 mice at 1 mg/kg or 5 mg/kg of body weight. Blood was collected over 28 days. Serum factor VII silencing was determined and normalized to that of control mice treated with PBS. Residual FVII levels were plotted against time for (A) 1 mg/kg and (B) 5 mg/kg siRNA. Results shown represent the mean ± s.d. of four animals.

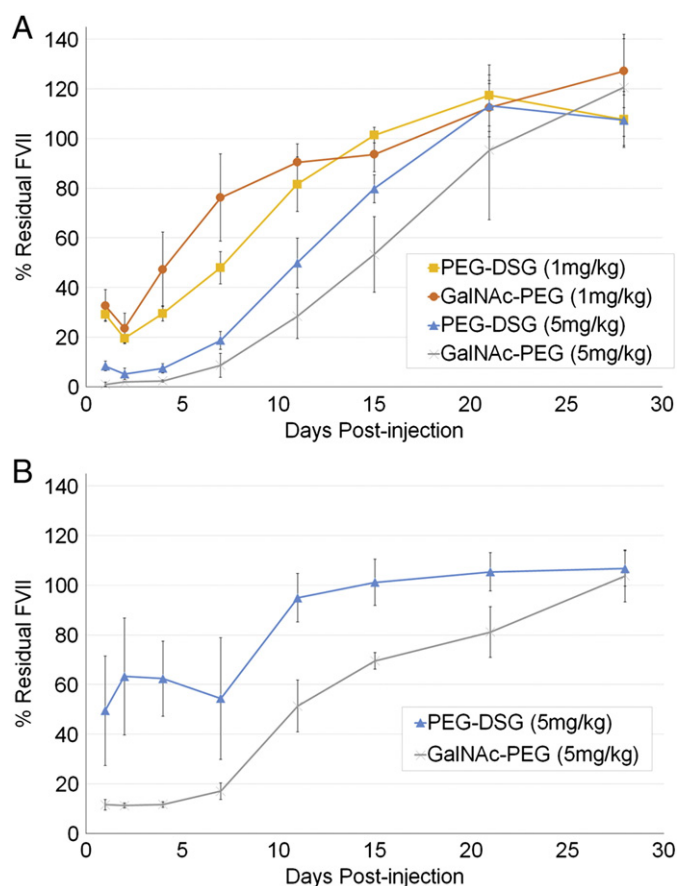


**Fig. 6.** Hepatic gene silencing can be enhanced using s.c. administered LNP-siRNA containing GalNAc-PEG lipid. (A) Mice were s.c. injected with ~45 nm PEG-DSG LNP with or without 0.5% GalNAc-PEG at 1 or 5 mg/kg siRNA. Residual FVII was monitored for 28 days. (B) Residual FVII was monitored over 28 days for animals injected with ~35 nm PEG-DSG or PEG-DSG with 0.5% GalNAc-PEG LNP. Results shown represent the mean  $\pm$  s.d. of four animals.

PEG-DMG LNP administered s.c. reached the circulation and virtually all of this material is subsequently accumulated in the liver, resulting in the levels observed 48 h post injection (Fig. 3B). It is noteworthy that although the ~30 nm PEG-DMG LNP had a low  $C_{max}$  and AUC in the blood, they showed relatively high accumulation in the liver further supporting a rapid hepatic clearance of PEG-DMG LNP that were drained into the blood. It is likely that at least 14% of the injected dose of the 30 nm PEG-DMG LNP reached the peripheral circulation. The rapid dissociation of PEG-DMG favours hepatocyte uptake while hindering drainage from the injection site. This may prove to be a useful aspect of LNP-siRNA *in vivo* behaviour as others have used particle aggregation as a strategy to promote liposome retention in lymph nodes [29]. It may be possible to modulate the rate of PEG-lipid dissociation by using different acyl anchor lengths such that an adequate quantity of LNP drains from the injection site while facilitating aggregation on reaching the lymph node.

When PEG-DMG was substituted with a more stable PEG-DSG, liver accumulation of LNP-siRNA was greatly enhanced. In the case of the ~45 nm diameter LNP, PEG-DSG LNP accumulated to levels three times higher than PEG-DMG LNP. This indicates that a stable PEG coating is an important factor, in addition to size, in allowing extravasation from the s.c. injection site to reach the liver, at least for the 30–80 nm size range tested here (Fig. 3B). Furthermore, all LNP made with PEG-DSG accumulate to similar levels (~15% of the injected dose) in the liver 48 h post injection while having drastically different maximum blood concentrations (2.7% for ~45 nm and 17.1% for ~30 nm). Finally, despite similar liver accumulation for PEG-DSG LNP systems (Fig. 3B),

differences in gene silencing were observed (Fig. 4B) suggesting that other factors in addition to tissue localization such as cellular uptake and endosome destabilization are involved in dictating LNP activity.

While a stable PEG-coat may prevent unwanted protein interactions and promote lymphatic drainage and circulation lifetimes, it is likely that this coat will impair LNP uptake into hepatocytes since this process requires the association of LNP with ApoE [12,13]. In this case, an exogenous targeting ligand such as GalNAc used in this study, can be tethered to the distal end of the PEG-lipid to enhance LNP uptake into target cells [12]. The incorporation of 0.5 mol.% of GalNAc-PEG greatly improved the activity of ~35 nm PEG-DSG LNP suggesting that inefficient cellular uptake was, in part, responsible for the reduction in activity of LNP containing PEG-DSG (Fig. 6B). Interestingly, the addition of GalNAc-PEG to larger ~45 nm systems did not improve the activity to the same extent as for smaller systems (Fig. 6A). This is presumably because LNP with 1.5 mol.% PEG-lipid are still able to associate with ApoE and the incorporation of an additional targeting ligand confers little additional benefit.

It is important to note that, regardless of the type of PEG-lipid coating, small LNP of size ~30 nm showed a reduction in activity compared to their larger counterparts (Fig. 4) despite showing favourable blood and liver accumulation following s.c. administration (Fig. 3). This presumably is due, in part, to inefficient release of the siRNA cargo from the endosome or a reduced siRNA and/or ionisable lipid payload per particle. Work is underway to investigate these factors and methods to improve efficacy of these small LNP-siRNA systems.

In addition to having rapid access to the circulation, small LNP, or LNP that have a stable PEG coating, also have the advantage of minimizing local immune responses at the site of injection. Indeed, signs of immune stimulation at the site of injection were observed for ~80 nm LNP containing the rapidly dissociable PEG-DMG. Mice injected with these relatively large particles showed lesions on the skin around the injection site (data not shown). Although the lesions resolved after one week, these possible immune-related responses raise concerns especially if high or repeat doses are required. It is possible that immunosuppressants could be co-administered to reduce the immune responses to LNP [30].

The work described in this study has significant implications for the development of LNP-siRNA to silence disease-causing genes *in vivo* following s.c. administration. An important reason for developing s.c. administrable drugs is the possibility of self-administration by patients. Previous work has shown that LNP-siRNA systems are well tolerated with therapeutic indices close to 1000 in rodents following i.v. injection [31,32]. However, the potency of LNP-siRNA systems delivered i.v. are significantly greater (~0.01 mg siRNA/kg body weight for 50% protein reduction) than achieved here for LNP-siRNA delivered s.c. (~1 mg siRNA/kg body weight for 50% protein reduction). As shown here, a major reason for this difference in potency is that a majority of s.c. administered material does not access the circulation. Smaller systems with stable PEG coatings that more readily extravasate to the circulation are less potent because of the presence of the stable PEG coat and an inherent lack of potency of smaller LNP-siRNA systems. To some extent this can be rectified by the inclusion of a targeting ligand such as GalNAc; however further gains in potency, in the range of a factor of 10, are necessary before s.c. administration of LNP-siRNA systems has clinical potential. This is because an injection volume of 10 mL/kg in rodents would translate to 800 mL for an 80 kg person. Assuming the maximum s.c. injection volume is ~2 mL, this would require 400 separate injections. To achieve an siRNA dose of 1 mg/kg for 2 mL injection volumes of the formulations employed here (0.1 mg siRNA/mL), the formulation would have to be concentrated to a lipid concentration of over 400 mg/mL, which is impractical.

As shown in this study, an important aspect of s.c. administration concerns enhanced delivery to the regional lymph nodes, particularly by small (~30 nm) systems. Methods of enhancing the gene silencing potency of these small LNP-siRNA systems are of interest and successful silencing of genes in immune cells in regional lymph could lead to treatments for inflammatory and autoimmune diseases as well as organ

rejection [33–35]. Also, tumour therapy would be expected to benefit from small LNP–siRNA systems of ~30 nm. Others have shown that small ~30 nm particles are able to penetrate into poorly permeable tumour tissue [36,37].

In summary, the work presented here is the first demonstration of LNP–siRNA mediated gene silencing in the liver following s.c. administration of LNP–siRNA systems over the size range of 30–80 nm with dissociable or stable PEG coatings. LNP–siRNA that are intermediate in size and ~45 nm in diameter exhibit maximum efficacy and with a dose as low as 1 mg/kg, greater than 50% hepatic gene silencing is observed and maintained over one week. Since small LNP size and a stable PEG coat appear to be essential for s.c. administration, future work will focus on improving the activity of small stably shielded LNP–siRNA. Other potential issues remain to be addressed to enable pre-clinical and clinical development of s.c. administered LNPs. These include potential injection site reactions caused by the LNPs or their components and the highly injection volumes required.

Supplementary data to this article can be found online at <http://dx.doi.org/10.1016/j.jconrel.2014.09.025>.

## Acknowledgements

This work was supported by the Canadian Institutes for Health Research (CIHR FRN 111627) and Alnylam Pharmaceuticals. We would also like to thank Martin Maier and Akin Akinc at Alnylam Pharmaceuticals for their feedback, Karen Lam for editing the manuscript and Yan Liu for technical assistance.

## References

- [1] Y. Tam, S. Chen, P. Cullis, Advances in lipid nanoparticles for siRNA delivery, *Pharmaceutics* 5 (2013) 498–507.
- [2] C. Wan, T.M. Allen, P.R. Cullis, Lipid nanoparticle delivery systems for siRNA-based therapeutics, *Drug Deliv. Transl. Res.* 1–10 (2013).
- [3] S.A. Barros, J.A. Gollob, Safety profile of RNAi nanomedicines, *Adv. Drug Deliv. Rev.* 64 (2012) 1730–1737.
- [4] C. Oussoren, G. Storm, Liposomes to target the lymphatics by subcutaneous administration, *Adv. Drug Deliv. Rev.* 50 (2001) 143–156.
- [5] T.M. Allen, C.B. Hansen, L.S. Guo, Subcutaneous administration of liposomes: a comparison with the intravenous and intraperitoneal routes of injection, *Biochim. Biophys. Acta* 1150 (1993) 9–16.
- [6] C. Oussoren, J. Zuidema, D.J. Crommelin, G. Storm, Lymphatic uptake and biodistribution of liposomes after subcutaneous injection. II. Influence of liposomal size, lipid composition and lipid dose, *Biochim. Biophys. Acta* 1328 (1997) 261–272.
- [7] C. Oussoren, G. Storm, Lymphatic uptake and biodistribution of liposomes after subcutaneous injection: III. Influence of surface modification with poly(ethylene glycol), *Pharm. Res.* 14 (1997) 1479–1484.
- [8] N.M. Belliveau, J. Huft, P.J.C. Lin, S. Chen, A.K.K. Leung, T.J. Leaver, A.W. Wild, J.B. Lee, R.J. Taylor, Y.K. Tam, C.L. Hansen, P.R. Cullis, Microfluidic synthesis of highly potent limit-size lipid nanoparticles for *In vivo* delivery of siRNA, *Mol. Ther. Nucleic Acids* 1 (2012) e37.
- [9] I.V. Zhigaltsev, N. Belliveau, I. Hafez, A.K. Leung, J. Huft, C. Hansen, P.R. Cullis, Bottom-up design and synthesis of limit size lipid nanoparticle systems with aqueous and triglyceride cores using millisecond microfluidic mixing, *Langmuir* 28 (2012) 3633–3640.
- [10] A.K. Leung, I.M. Hafez, S. Baoukina, N.M. Belliveau, I.V. Zhigaltsev, E. Afshinmanesh, D.P. Tieleman, C.L. Hansen, M.J. Hope, P.R. Cullis, Lipid nanoparticles containing siRNA synthesized by microfluidic mixing exhibit an electron-dense nanostructured core, *J. Phys. Chem. C Nanomater. Interfaces* 116 (2012) 18440–18450.
- [11] B.L. Mui, Y.K. Tam, M. Jayaraman, S.M. Ansell, X. Du, Y.Y. Tam, P.J. Lin, S. Chen, J.K. Narayanannair, K.G. Rajeev, M. Manoharan, A. Akinc, M.A. Maier, P. Cullis, T.D. Madden, M.J. Hope, Influence of polyethylene glycol lipid desorption rates on pharmacokinetics and pharmacodynamics of siRNA lipid nanoparticles, *Mol. Ther. Nucleic Acids* 2 (2013) e139.
- [12] A. Akinc, W. Querbes, S. De, J. Qin, M. Frank-Kamenetsky, K.N. Jayaprakash, M. Jayaraman, K.G. Rajeev, W.L. Cantley, J.R. Dorkin, J.S. Butler, L. Qin, T. Racie, A. Sprague, E. Fava, A. Zeiger, M.J. Hope, M. Zerial, D.W. Sah, K. Fitzgerald, M.A. Tracy, M. Manoharan, V. Kotliansky, A. Fougerolles, M.A. Maier, Targeted delivery of RNAi therapeutics with endogenous and exogenous ligand-based mechanisms, *Mol. Ther.* 18 (2010) 1357–1364.
- [13] X. Yan, F. Kuipers, L.M. Havekes, R. Havinga, B. Dontje, K. Poelstra, G.L. Scherphof, J.A. Kamps, The role of apolipoprotein E in the elimination of liposomes from blood by hepatocytes in the mouse, *Biochim. Biophys. Res. Commun.* 328 (2005) 57–62.
- [14] J.A. Kamps, G.L. Scherphof, Receptor versus non-receptor mediated clearance of liposomes, *Adv. Drug Deliv. Rev.* 32 (1998) 81–97.
- [15] P.C. Rensen, L.A. Sliedregt, M. Ferns, E. Kieviet, S.M. van Rossenberg, S.H. van Leeuwen, T.J. van Berkel, E.A. Biessen, Determination of the upper size limit for uptake and processing of ligands by the asialoglycoprotein receptor on hepatocytes *in vitro* and *in vivo*, *J. Biol. Chem.* 276 (2001) 37577–37584.
- [16] P.C. Rensen, S.H. van Leeuwen, L.A. Sliedregt, T.J. van Berkel, E.A. Biessen, Design and synthesis of novel N-acetylgalactosamine-terminated glycolipids for targeting of lipoproteins to the hepatic asialoglycoprotein receptor, *J. Med. Chem.* 47 (2004) 5798–5808.
- [17] A. Ciechanover, A.L. Schwartz, H.F. Lodish, The asialoglycoprotein receptor internalizes and recycles independently of the transferrin and insulin receptors, *Cell* 32 (1983) 267–275.
- [18] P.C. Rensen, L.A. Sliedregt, P.J. van Santbrink, M. Ferns, H.N. Schifferstein, S.H. van Leeuwen, J.H. Souverijn, T.J. van Berkel, E.A. Biessen, Stimulation of liver-directed cholesterol flux in mice by novel N-acetylgalactosamine-terminated glycolipids with high affinity for the asialoglycoprotein receptor, *Arterioscler. Thromb. Vasc. Biol.* 26 (2006) 169–175.
- [19] R.L. Rungta, H.B. Choi, P.J. Lin, R.W. Ko, D. Ashby, J. Nair, M. Manoharan, P.R. Cullis, B.A. Macvicar, Lipid nanoparticle delivery of siRNA to silence neuronal gene expression in the brain, *Mol. Ther. Nucleic Acids* 2 (2013) e136.
- [20] A. Akinc, A. Zumbuehl, M. Goldberg, E.S. Leshchiner, V. Busini, N. Hossain, S.A. Bacallado, D.N. Nguyen, J. Fuller, R. Alvarez, A. Borodovsky, T. Borland, R. Constien, A. de Fougerolles, J.R. Dorkin, K. Narayanannair Jayaprakash, M. Jayaraman, M. John, V. Kotliansky, M. Manoharan, L. Nechev, J. Qin, T. Racie, D. Raitcheva, K.G. Rajeev, D.W. Sah, J. Soutschek, I. Toudjarska, H.P. Vornlocher, T.S. Zimmermann, R. Langer, D.G. Anderson, A combinatorial library of lipid-like materials for delivery of RNAi therapeutics, *Nat. Biotechnol.* 26 (2008) 561–569.
- [21] S.C. Semple, A. Akinc, J. Chen, A.P. Sandhu, B.L. Mui, C.K. Cho, D.W. Sah, D. Stebbing, E.J. Crosley, E. Yaworski, I.M. Hafez, J.R. Dorkin, J. Qin, K. Lam, K.G. Rajeev, K.F. Wong, L.B. Jeffs, L. Nechev, M.L. Eisenhardt, M. Jayaraman, M. Kazem, M.A. Maier, M. Srinivasulu, M.J. Weinstein, Q. Chen, R. Alvarez, S.A. Barros, S. De, S.K. Klimuk, T. Borland, V. Kosovrasti, W.L. Cantley, Y.K. Tam, M. Manoharan, M.A. Ciufolini, M.A. Tracy, A. de Fougerolles, I. MacLachlan, P.R. Cullis, T.D. Madden, M.J. Hope, Rational design of cationic lipids for siRNA delivery, *Nat. Biotechnol.* 28 (2010) 172–176.
- [22] A. Akinc, M. Goldberg, J. Qin, J.R. Dorkin, C. Gamba-Vitalo, M. Maier, K.N. Jayaprakash, M. Jayaraman, K.G. Rajeev, M. Manoharan, V. Kotliansky, I. Rohl, E.S. Leshchiner, R. Langer, D.G. Anderson, Development of lipidoid-siRNA formulations for systemic delivery to the liver, *Mol. Ther.* 17 (2009) 872–879.
- [23] S.C. Semple, T.O. Harasym, K.A. Clow, S.M. Ansell, S.K. Klimuk, M.J. Hope, Immunogenicity and rapid blood clearance of liposomes containing polyethylene glycol-lipid conjugates and nucleic acid, *J. Pharmacol. Exp. Ther.* 312 (2005) 1020–1026.
- [24] N.L. Tilney, Patterns of lymphatic drainage in the adult laboratory rat, *J. Anat.* 109 (1971) 369–383.
- [25] P.R. Cullis, A. Chonn, S.C. Semple, Interactions of liposomes and lipid-based carrier systems with blood proteins: Relation to clearance behaviour *in vivo*, *Adv. Drug Deliv. Rev.* 32 (1998) 3–17.
- [26] T.M. Allen, C. Hansen, F. Martin, C. Redemann, A. Yau-Young, Liposomes containing synthetic lipid derivatives of poly(ethylene glycol) show prolonged circulation half-lives *in vivo*, *Biochim. Biophys. Acta* 1066 (1991) 29–36.
- [27] M.C. Woodle, D.D. Lasic, Sterically stabilized liposomes, *Biochim. Biophys. Acta* 1113 (1992) 171–199.
- [28] M.J. Hope, M.B. Bally, L.D. Mayer, A.S. Janoff, P.R. Cullis, Generation of multilamellar and unilamellar phospholipid vesicles, *Chem. Phys. Lipids* 40 (1986) 89–107.
- [29] W.T. Phillips, R. Klipper, B. Goins, Novel method of greatly enhanced delivery of liposomes to lymph nodes, *J. Pharmacol. Exp. Ther.* 295 (2000) 309–313.
- [30] M.T. Abrams, M.L. Koser, J. Seitzer, S.C. Williams, M.A. DiPietro, W. Wang, A.W. Shaw, X. Mao, V. Jadhav, J.P. Davide, P.A. Burke, A.B. Sachs, S.M. Stirdivant, L. Sepp-Lorenzino, Evaluation of efficacy, biodistribution, and inflammation for a potent siRNA nanoparticle: effect of dexamethasone co-treatment, *Mol. Ther.* 18 (2010) 171–180.
- [31] M. Jayaraman, S.M. Ansell, B.L. Mui, Y.K. Tam, J. Chen, X. Du, D. Butler, L. Eltepu, S. Matsuda, J.K. Narayanannair, K.G. Rajeev, I.M. Hafez, A. Akinc, M.A. Maier, M.A. Tracy, P.R. Cullis, T.D. Madden, M. Manoharan, M.J. Hope, Maximizing the potency of siRNA lipid nanoparticles for hepatic gene silencing *in vivo*, *Angew. Chem. Int. Ed. Engl.* 51 (2012) 8529–8533.
- [32] M.A. Maier, M. Jayaraman, S. Matsuda, J. Liu, S. Barros, W. Querbes, Y.K. Tam, S.M. Ansell, V. Kumar, J. Qin, X. Zhang, Q. Wang, S. Panesar, R. Hutabarat, M. Carioto, J. Hettinger, P. Kandasamy, D. Butler, K.G. Rajeev, B. Pang, K. Charisse, K. Fitzgerald, B.L. Mui, X. Du, P. Cullis, T.D. Madden, M.J. Hope, M. Manoharan, A. Akinc, Biodegradable lipids enabling rapidly eliminated lipid nanoparticles for systemic delivery of RNAi therapeutics, *Mol. Ther.* 21 (2013) 1570–1578.
- [33] T.E. Ichim, R. Zhong, W.P. Min, Prevention of allograft rejection by *in vitro* generated tolerogenic dendritic cells, *Transpl. Immunol.* 11 (2003) 295–306.
- [34] J.A. Hill, T.E. Ichim, K.P. Kusznieruk, M. Li, X. Huang, X. Yan, R. Zhong, E. Cairns, D.A. Bell, W.P. Min, Immune modulation by silencing IL-12 production in dendritic cells using small interfering RNA, *J. Immunol.* 171 (2003) 691–696.
- [35] X. Zheng, C. Vladau, X. Zhang, M. Suzuki, T.E. Ichim, Z.X. Zhang, M. Li, E. Carrier, B. Garcia, A.M. Jevnikar, W.P. Min, A novel *in vivo* siRNA delivery system specifically targeting dendritic cells and silencing CD40 genes for immunomodulation, *Blood* 113 (2009) 2646–2654.
- [36] H. Cabral, Y. Matsumoto, K. Mizuno, Q. Chen, M. Murakami, M. Kimura, Y. Terada, M.R. Kano, K. Miyazono, M. Uesaka, N. Nishiyama, K. Kataoka, Accumulation of sub-100 nm polymeric micelles in poorly permeable tumours depends on size, *Nat. Nanotechnol.* 6 (2011) 815–823.
- [37] S. Huo, H. Ma, K. Huang, J. Liu, T. Wei, S. Jin, J. Zhang, S. He, X.J. Liang, Superior penetration and retention behavior of 50 nm gold nanoparticles in tumors, *Cancer Res.* 73 (2013) 319–330.